


Few-Body Syst (2016) 57:1213–1225  
DOI 10.1007/s00601-016-1156-3



H. Witała  · J. Golak · R. Skibiński · K. Topolnicki ·  
E. Epelbaum · K. Hebeler · H. Kamada · H. Krebs ·  
U.-G. Meißner · A. Nogga

## Role of the Total Isospin $3/2$ Component in Three-Nucleon Reactions

Received: 6 May 2016 / Accepted: 6 September 2016 / Published online: 5 October 2016  
© The Author(s) 2016. This article is published with open access at Springerlink.com

**Abstract** We discuss the role of the three-nucleon isospin  $T = 3/2$  amplitude in elastic neutron–deuteron scattering and in the deuteron breakup reaction. The contribution of this amplitude originates from charge-independence breaking of the nucleon–nucleon potential and is driven by the difference between neutron–neutron (proton–proton) and neutron–proton forces. We study the magnitude of that contribution to the elastic scattering and breakup observables, taking the locally regularized chiral  $N^4$ LO nucleon–nucleon potential supplemented by the chiral  $N^2$ LO three-nucleon force. For comparison we employ also the Av18 nucleon–nucleon potential combined with the Urbana IX three-nucleon force. We find that the isospin  $T = 3/2$  component is important for the breakup reaction and the proper treatment of charge-independence breaking in this case requires the inclusion of the  $^1S_0$  state with isospin  $T = 3/2$ . For neutron–deuteron elastic scattering the  $T = 3/2$  contributions are insignificant and charge-independence breaking can be accounted for by using the effective t-matrix generated with the so-called “ $2/3 - 1/3$ ” rule.

This article belongs to the special issue “30th anniversary of Few-Body Systems”.

H. Witała (✉) · J. Golak · R. Skibiński · K. Topolnicki  
M. Smoluchowski Institute of Physics, Jagiellonian University, 30348 Kraków, Poland  
E-mail: henryk.witala@uj.edu.pl

E. Epelbaum · H. Krebs  
Institut für Theoretische Physik II, Ruhr-Universität Bochum, 44780 Bochum, Germany

K. Hebeler  
Institut für Kernphysik, Technische Universität Darmstadt, 64289 Darmstadt, Germany

K. Hebeler  
Extreme Matter Institute EMMI, GSI Helmholtzzentrum für Schwerionenforschung GmbH, 64291 Darmstadt, Germany

H. Kamada  
Department of Physics, Faculty of Engineering, Kyushu Institute of Technology, Kitakyushu 804-8550, Japan

U.-G. Meißner  
Helmholtz-Institut für Strahlen- und Kernphysik and Bethe Center for Theoretical Physics, Universität Bonn, 53115 Bonn, Germany

U.-G. Meißner  
Institute for Advanced Simulation, Institut für Kernphysik, Jülich Center for Hadron Physics, and JARA - High Performance Computing, Forschungszentrum Jülich, 52425 Jülich, Germany

A. Nogga  
Institut für Kernphysik, Institute for Advanced Simulation and Jülich Center for Hadron Physics, Forschungszentrum Jülich, 52425 Jülich, Germany

## 1 Introduction

Charge-independence breaking (CIB) is well established in the two-nucleon (2N) system in the  $^1S_0$  state as evidenced by the values of the scattering lengths  $-23.75 \pm 0.01$ ,  $-17.3 \pm 0.8$ , and  $-18.5 \pm 0.3$  fm [1,2] for the neutron–proton (np), proton–proton (pp) (with the Coulomb force subtracted), and neutron–neutron (nn) systems, respectively. That knowledge of CIB is incorporated into modern, high precision NN potentials, as exemplified by the standard semi-phenomenological models: Av18 [3], CD Bonn [4], or NijmI and NijmII [5], as well as by the chiral NN forces [6–8]. Treating neutrons and protons as identical particles requires that nuclear systems are described not only in terms of the momentum and spin but also isospin states. The general classification of the isospin dependence of the NN force is given in [9]. The isospin violating 2N forces induce an admixture of the total isospin  $T = 3/2$  state to the dominant  $T = 1/2$  state in the three-nucleon (3N) system. The CIB of the NN interaction thus affects 3N observables. The detailed treatment of the 3N system with CIB NN forces in the case of distinguishable or identical particles was formulated and described in [10]. We extend the investigation done in [10] by including a three-nucleon force (3NF). In the calculations performed with the standard semi-phenomenological potentials we use the UrbanaIX (UIX) [11] 3NF, while the chiral  $N^2$ LO 3N force [12] is used in addition to the recent and most accurate chiral NN interactions [13,14]. In this paper, based on such dynamics, we discuss the role of the amplitude with the total three-nucleon (3N) isospin  $T = 3/2$  in elastic neutron–deuteron (nd) scattering and in the corresponding breakup reaction. In Sect. 2 we briefly describe the formalism of 3N continuum Faddeev calculations and the inclusion of CIB. The results are presented in Sect. 3. In Sect. 3.1 we discuss our results for elastic nd scattering and in Sect. 3.2 describe our findings for selected breakup configurations. We summarize and conclude in Sect. 4.

## 2 3N Scattering and Charge Independence Breaking

Neutron–deuteron scattering with nucleons interacting through a NN interaction  $v_{NN}$  and a 3NF  $V_{123}$ , is described in terms of a breakup operator  $T$  satisfying the Faddeev-type integral equation [15–17]

$$T|\phi\rangle = tP|\phi\rangle + (1 + tG_0)V^{(1)}(1 + P)|\phi\rangle + tPG_0T|\phi\rangle + (1 + tG_0)V^{(1)}(1 + P)G_0T|\phi\rangle. \quad (1)$$

The two-nucleon  $t$ -matrix  $t$  is the solution of the Lippmann–Schwinger equation with the interaction  $v_{NN}$ .  $V^{(1)}$  is the part of a 3NF which is symmetric under the interchange of nucleons 2 and 3:  $V_{123} = V^{(1)}(1 + P)$ . The permutation operator  $P = P_{12}P_{23} + P_{13}P_{23}$  is given in terms of the transposition operators,  $P_{ij}$ , which interchange nucleons  $i$  and  $j$ . The incoming state  $|\phi\rangle = |\mathbf{q}_0\rangle|\phi_d\rangle$  describes the free relative motion of the neutron and the deuteron with the relative momentum  $\mathbf{q}_0$  and contains the internal deuteron state  $|\phi_d\rangle$ . Finally,  $G_0$  is the resolvent of the three-body center-of-mass kinetic energy. The amplitude for elastic scattering leading to the corresponding two-body final state  $|\phi'\rangle$  is then given by [16,17]

$$\langle\phi'|U|\phi\rangle = \langle\phi'|PG_0^{-1}|\phi\rangle + \langle\phi'|PT|\phi\rangle + \langle\phi'|V^{(1)}(1 + P)|\phi\rangle + \langle\phi'|V^{(1)}(1 + P)G_0T|\phi\rangle, \quad (2)$$

while for the breakup reaction one has

$$\langle\phi'_0|U_0|\phi\rangle = \langle\phi'_0|(1 + P)T|\phi\rangle, \quad (3)$$

where  $|\phi'_0\rangle$  is the free three-body breakup channel state.

Solving Eq. (1) in the momentum-space partial wave basis, defined by the magnitudes of the 3N Jacobi momenta  $p$  and  $q$  [16] together with the angular momenta, spin and isospin quantum numbers  $\alpha$  ( $\beta$ ) [16], is performed by projecting Eq. (1) onto two types of basis states:

$$|pq\alpha\rangle \equiv |pq \text{ angular momenta spins}\rangle \left(t\frac{1}{2}\right) T = \frac{1}{2}M_T, \quad (t = 0, 1), \quad (4)$$

and

$$|pq\beta\rangle \equiv |pq \text{ angular momenta spins}\rangle \left(t\frac{1}{2}\right) T = \frac{3}{2}M_T, \quad (t = 1). \quad (5)$$

Assuming charge conservation and employing the notation where the neutron (proton) isospin projection is  $\frac{1}{2}$  ( $-\frac{1}{2}$ ), the 2N t-operator in the three-particle isospin space can be decomposed for the nd system as [10]:

$$\begin{aligned} \left\langle \left( t \frac{1}{2} \right) T M_T = \frac{1}{2} \middle| t \left( t' \frac{1}{2} \right) T' M_{T'} = \frac{1}{2} \right\rangle &= \delta_{t t'} \delta_{T T'} \delta_{T 1/2} \left[ \delta_{t 0} t_{np}^{t=0} + \delta_{t 1} \left( \frac{2}{3} t_{nn}^{t=1} + \frac{1}{3} t_{np}^{t=1} \right) \right] \\ &+ \delta_{t t'} \delta_{t 1} (1 - \delta_{T T'}) \frac{\sqrt{2}}{3} (t_{nn}^{t=1} - t_{np}^{t=1}) \\ &+ \delta_{t t'} \delta_{t 1} \delta_{T T'} \delta_{T 3/2} \left( \frac{1}{3} t_{nn}^{t=1} + \frac{2}{3} t_{np}^{t=1} \right), \end{aligned} \quad (6)$$

where  $t_{nn}$  and  $t_{np}$  are solutions of the Lippman–Schwinger equations driven by the  $v_{nn}$  and  $v_{np}$  potentials, respectively.

As a result of solving Eq. (1) one gets the amplitudes  $\langle pq\alpha|T|\phi\rangle$  and  $\langle pq\beta|T|\phi\rangle$ , which fulfill the following set of coupled integral equations:

$$\begin{aligned} \langle pq\alpha|T|\phi\rangle &= \sum_{\alpha'} \int_{p'q'} \langle pq\alpha|t|p'q'\alpha'\rangle \langle p'q'\alpha'|P|\phi\rangle \\ &+ \sum_{\alpha'} \int_{p'q'} \langle pq\alpha|V^{(1)}|p'q'\alpha'\rangle \langle p'q'\alpha'|(1+P)|\phi\rangle \\ &+ \sum_{\alpha'} \int_{p'q'} \langle pq\alpha|t|p'q'\alpha'\rangle \langle p'q'\alpha'|G_0V^{(1)}(1+P)|\phi\rangle \\ &+ \sum_{\alpha'} \int_{p'q'} \langle pq\alpha|t|p'q'\alpha'\rangle \langle p'q'\alpha'|PG_0T|\phi\rangle \\ &+ \sum_{\beta'} \int_{p'q'} \langle pq\alpha|t|p'q'\beta'\rangle \langle p'q'\beta'|PG_0T|\phi\rangle \\ &+ \sum_{\alpha'} \int_{p'q'} \langle pq\alpha|V^{(1)}|p'q'\alpha'\rangle \langle p'q'\alpha'|(1+P)G_0T|\phi\rangle \\ &+ \sum_{\alpha'} \int_{p'q'} \sum_{\alpha''} \int_{p''q''} \langle pq\alpha|t|p'q'\alpha'\rangle \langle p'q'\alpha'|G_0V^{(1)}|p''q''\alpha''\rangle \\ &\times \langle p''q''\alpha''|(1+P)G_0T|\phi\rangle \\ &+ \sum_{\beta'} \int_{p'q'} \sum_{\beta''} \int_{p''q''} \langle pq\alpha|t|p'q'\beta'\rangle \langle p'q'\beta'|G_0V^{(1)}|p''q''\beta''\rangle \\ &\times \langle p''q''\beta''|(1+P)G_0T|\phi\rangle \\ \langle pq\beta|T|\phi\rangle &= \sum_{\alpha'} \int_{p'q'} \langle pq\beta|t|p'q'\alpha'\rangle \langle p'q'\alpha'|P|\phi\rangle \\ &+ \sum_{\alpha'} \int_{p'q'} \langle pq\beta|t|p'q'\alpha'\rangle \langle p'q'\alpha'|G_0V^{(1)}(1+P)|\phi\rangle \\ &+ \sum_{\alpha'} \int_{p'q'} \langle pq\beta|t|p'q'\alpha'\rangle \langle p'q'\alpha'|PG_0T|\phi\rangle \\ &+ \sum_{\beta'} \int_{p'q'} \langle pq\beta|t|p'q'\beta'\rangle \langle p'q'\beta'|PG_0T|\phi\rangle \\ &+ \sum_{\beta'} \int_{p'q'} \langle pq\beta|V^{(1)}|p'q'\beta'\rangle \langle p'q'\beta'|(1+P)G_0T|\phi\rangle \\ &+ \sum_{\alpha'} \int_{p'q'} \sum_{\alpha''} \int_{p''q''} \langle pq\beta|t|p'q'\alpha'\rangle \langle p'q'\alpha'|G_0V^{(1)}|p''q''\alpha''\rangle \end{aligned}$$

$$\begin{aligned}
& \times \langle p'' q'' \alpha'' | (1 + P) G_0 T | \phi \rangle \\
& + \sum_{\beta'} \int_{p' q'} \sum_{\beta''} \int_{p'' q''} \langle p q \beta | t | p' q' \beta' \rangle \langle p' q' \beta' | G_0 V^{(1)} | p'' q'' \beta'' \rangle \\
& \times \langle p'' q'' \beta'' | (1 + P) G_0 T | \phi \rangle .
\end{aligned}$$

The form of the couplings in Eq. (7) follows from the fact that the incoming neutron–deuteron state  $|\phi\rangle$  is a total isospin  $T = 1/2$  state, the permutation operator  $P$  is diagonal in the total isospin, and the 3NF is assumed to conserve the total isospin  $T$  [18].

From Eq. (7) it is clear that only when the nn and np interactions differ in the same orbital and spin angular-momentum states with the 2N subsystem isospin  $t = 1$  (CIB), then the amplitudes  $\langle p q \beta | T | \phi \rangle$  will be nonzero. In addition, their magnitude is driven by the strength of the CIB as given by the difference of the corresponding t-matrices  $\frac{\sqrt{2}}{3}(t_{nn}^{t=1} - t_{np}^{t=1})$  in Eq. (6). In such a case, not only the magnitude of CIB decides about the importance of the  $\langle p q \beta | T | \phi \rangle$  contributions, but also the isospin  $T = 3/2$  3NF matrix elements, which participate in generating the  $\langle p q \beta | T | \phi \rangle$  amplitudes. It is the set of equations Eq. (7) which we solve when we differentiate between nn and np interactions and include both  $T = 1/2$  and  $T = 3/2$  3NF matrix elements.

In the case when the neglect of the  $T = 3/2$  amplitudes  $\langle p q \beta | T | \phi \rangle$  is justified, the CIB can be taken care of by using the effective two-body t-matrix generated with the so-called “2/3 – 1/3” rule,  $t_{\text{eff}} = \frac{2}{3}t_{nn}^{t=1} + \frac{1}{3}t_{np}^{t=1}$ , see Eq. (6), in the 2N subsystem isospin  $t = 1$  states and restricting the treatment only to the amplitudes  $\langle p q \alpha | T | \phi \rangle$ .

Since the final state  $|\phi'\rangle$  in elastic nd scattering also has the total 3N isospin  $T = 1/2$ , the amplitudes  $\langle p q \beta | T | \phi \rangle$  do not contribute directly to this reaction. The  $T = 3/2$  admixture enters in this case through a modification of the  $T = 1/2$  amplitudes  $\langle p q \alpha | T | \phi \rangle$  induced by the couplings given in Eq. (7). Contrary to that, for the nd breakup reaction both  $T = 1/2$  ( $\langle p q \alpha | T | \phi \rangle$ ) and  $T = 3/2$  ( $\langle p q \beta | T | \phi \rangle$ ) amplitudes contribute.

### 3 Results

In order to check the importance of the isospin  $T = 3/2$  contributions we solved the 3N Faddeev equations Eq. (7) for four values of the incoming neutron laboratory energy:  $E_{\text{lab}} = 13, 65, 135,$  and  $250$  MeV. As a NN potential we took the semi-locally regularized N<sup>4</sup>LO chiral potential of Ref. [13,14,19] with the regulator  $R = 0.9$  fm, alone or combined with the chiral N<sup>2</sup>LO 3NF [12,20], regularized with the same regulator. We additionally regularized matrix elements of that 3NF by multiplying it with a nonlocal regulator  $f(p, q) = \exp\{-(p^2 + \frac{3}{4}q^2)^3/\Lambda^6\}$  with large cut-off value  $\Lambda = 1000$  MeV. This additional regulator is applied to the 3NF matrix elements only for technical reasons. The practical calculation of the local 3NFs involve the evaluation of convolution integrals whose calculation becomes numerically unstable at very large momenta. The value of the cutoff scale  $\Lambda$  is chosen sufficiently large so that low-energy physics is not affected by this additional regulator. In fact, we have checked explicitly that the effects of this regulator for the chosen cutoff value are negligible in three-body bound state and scattering calculations. As a nn force we took the pp version of that particular NN interaction (with the Coulomb force subtracted). The low-energy constants of the contact interactions in that 3NF were adjusted to the triton binding energy [12] and we used  $c_D = 6.0$  for the one-pion exchange contribution and  $c_E = -1.0943$  for the 3N contact term (we are using the notation of Ref. [12] with  $\Lambda = 700$  MeV). That specific choice of the  $c_D$  and  $c_E$  values does not only reproduce the experimental triton binding energy when that N<sup>4</sup>LO NN and N<sup>2</sup>LO 3NF are combined but also improves description of the nucleon–deuteron elastic scattering cross section data at higher energies (see Fig. 4a) comparable to that obtained by combining realistic NN interactions with standard models of 3NF’s [21,22]. In order to provide convergent predictions we solved Eq. (7) taking into account all partial wave states with the total 2N angular momenta up to  $j_{\text{max}} = 5$  and 3N total angular momenta up to  $J_{\text{max}} = 25/2$ . The 3NF was included up to  $J_{\text{max}} = 7/2$ .

We present results for that particular combination of the chiral NN and 3N forces (of course, in the future a more consistent set of 2N and 3N forces needs to be employed, once the corresponding 3NFs are available). However, we checked using the example of the Av18 and Urbana IX 3NF combination that the conclusions remain unchanged when instead of the chiral forces so-called high precision realistic forces are used.

Since CIB effects are driven by the difference between np and nn t-matrices we display in Figs. 1 and 2 for the  $^1S_0$  and  $^3P_0$  NN partial waves, respectively, the np t-matrix  $t_{np}(p, p'; E - \frac{3}{4}q^2)$  (a) and the difference

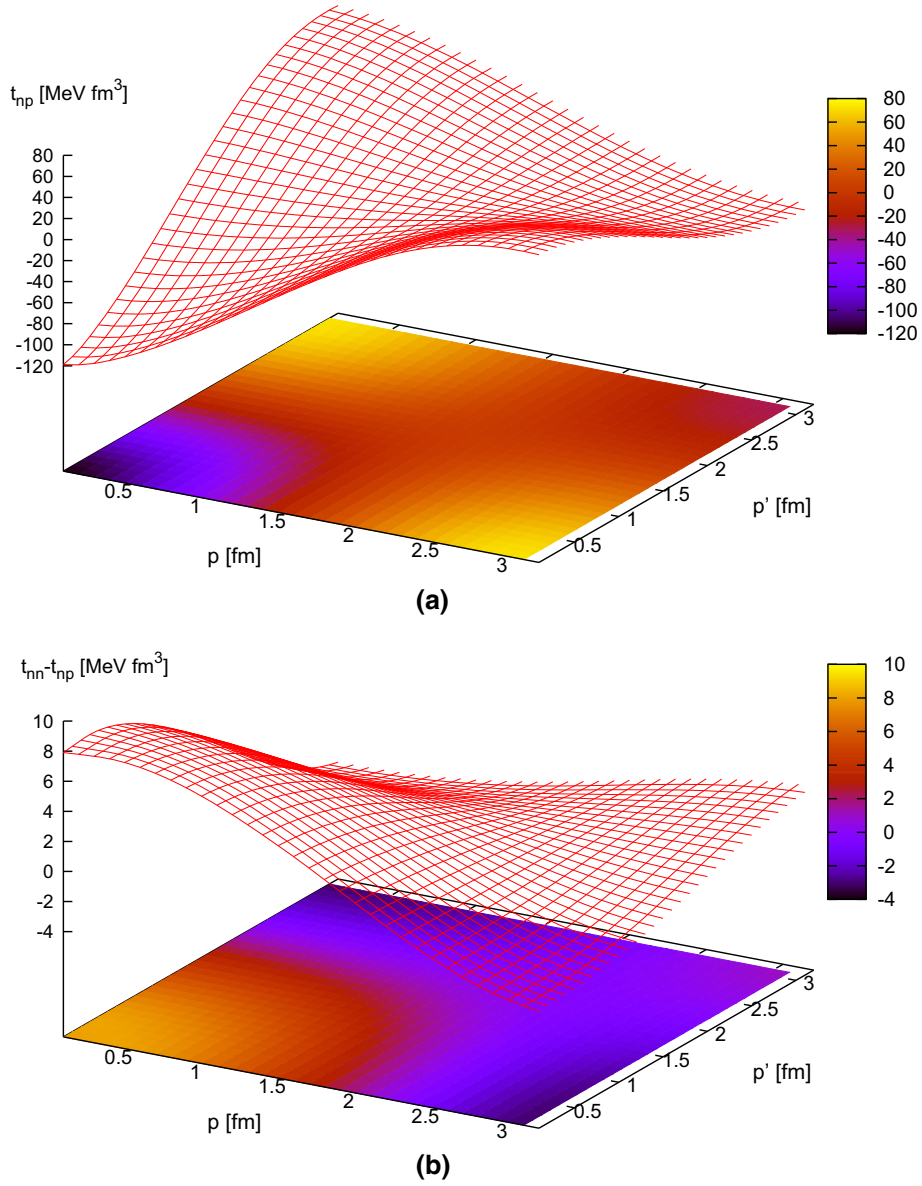


**Fig. 1** (Color online) The np t-matrix  $t_{np}(p, p'; E - \frac{3}{4}q^2)$  (a) and the difference of the nn and np t-matrices (b) at incoming neutron laboratory energy  $E_{lab} = 13$  MeV for the  $^1S_0$  partial wave, as a function of the relative NN momenta  $p$  and  $p'$  at a particular value of the spectator nucleon momentum  $q = 0.528$  fm $^{-1}$  at which the 2N subsystem energy is equal to the binding energy of the deuteron  $E_d$ :  $E - \frac{3}{4}q^2 = E_d$

$t_{np}(p, p'; E - \frac{3}{4}q^2) - t_{nn}(p, p'; E - \frac{3}{4}q^2)$  (b), at the laboratory energy of the incoming neutron  $E_{lab} = 13$  MeV. They are displayed as a function of the NN relative momenta  $p$  and  $p'$  for a chosen value of the spectator nucleon momentum  $q = 0.528$  fm $^{-1}$  at which the 2N subsystem energy is equal to the binding energy of the deuteron  $E_d$ :  $E - \frac{3}{4}q^2 = E_d$ . The behaviour of the  $t_{np}$  as well as of the difference  $t_{np} - t_{nn}$  is similar at other energies. It is interesting to note that the difference between the np and nn t-matrices ranges up to  $\approx 10\%$ .

In Tables 1, 2, and 3 we show at the chosen energies the total cross section for the nd interaction, the total nd elastic scattering cross section, and the total nd breakup cross section, respectively, calculated with different underlying dynamics based on the chiral N $^4$ LO NN or/and N $^2$ LO 3NF force. Namely, the results in column 2 of those tables (no CIB,  $V_{123} = 0$ ,  $^1S_0$  np) were obtained with the NN force only, assuming no CIB and using in all  $t = 1$  partial waves the effective t-matrix  $t_{eff} = (2/3)t_{nn} + (1/3)t_{np}$ , with the exception of the  $^1S_0$  partial wave, where only the np force was taken.

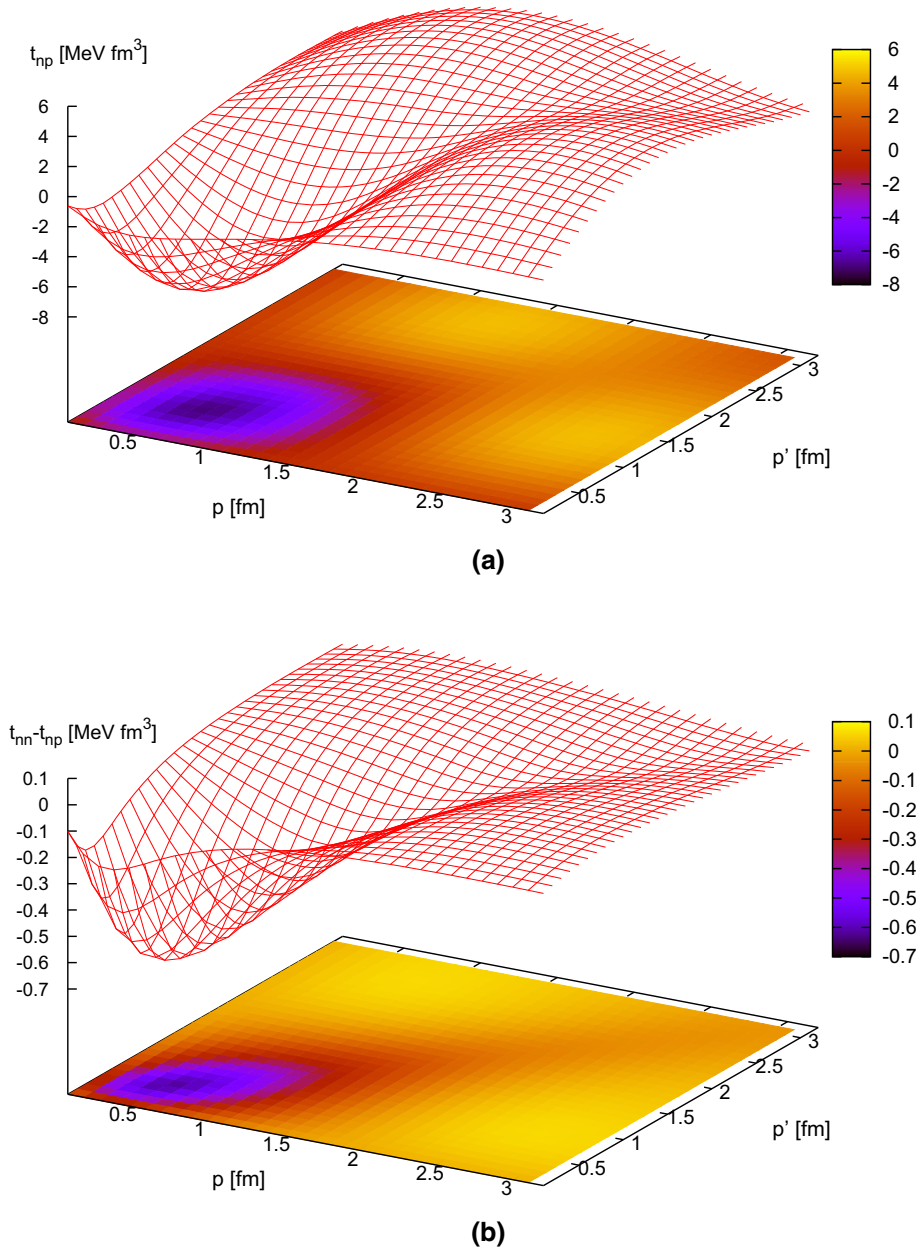


**Fig. 2** (Color online) The same as in Fig. 1 but for the  $^3P_0$  partial wave

In column 3 instead of the np  $^1S_0$  NN force a nn one was taken (no CIB,  $V_{123} = 0$ ,  $^1S_0$  nn). In column 4 in all  $t = 1$  partial waves (including also  $^1S_0$  one) only  $T = 1/2$  was taken into account and the effective t-matrix  $t_{\text{eff}} = (2/3)t_{nn} + (1/3)t_{np}$  was used (no CIB,  $V_{123} = 0$ ,  $t_{\text{eff}}$ ). In column 5 the NN interaction of column 4 was combined with 3NF (no CIB,  $V_{123}$ ,  $t_{\text{eff}}$ ). In column 6 a proper treatment of the CIB in the  $^1S_0$  partial wave was performed by taking in that partial wave both np and nn interactions and keeping in addition to the total isospin  $T = 1/2$  also  $T = 3/2$ . In all other  $t = 1$  states the effective t-matrix  $t_{\text{eff}}$  was used and only states with  $T = 1/2$  were kept. No 3NF was allowed ( $^1S_0$  CIB,  $V_{123} = 0$ ). The proper treatment of CIB in all states with  $t = 1$ , when both np and nn interactions were used and both  $T = 1/2$  and  $T = 3/2$  states were kept, are shown in column 8 and 9 for the cases when NN interactions were used alone (CIB,  $V_{123} = 0$ ) and combined with 3NF (CIB,  $V_{123}$ ), respectively.

**Table 1** The nd total cross section (in [mb]) at energies given in the first column. Dynamical models related to the particular columns are: in 2nd, 3rd, 4th, and 5th no CIB in any  $t = 1$  states was assumed. In the  $^1S_0$  state the t-matrix has been taken as  $t_{np}$  and  $t_{nn}$  for the 2nd and 3rd, and as  $t_{\text{eff}} = (2/3)t_{nn} + (1/3)t_{np}$  for the 4th and 5th. In all other  $t = 1$  states  $t_{\text{eff}}$  was used. Descriptions  $V_{123} = 0$  and  $V_{123}$  means that the NN interaction was taken alone and combined with the 3NF, respectively. In the 6th and 7th columns CIB was exactly taken into account by using in  $^1S_0$  state both  $t_{np}$  and  $t_{nn}$  t-matrices and state with isospin  $T = 3/2$  was taken into account. In all other  $t = 1$  states effective t-matrix  $t_{\text{eff}}$  was used. In the 8th and 9th columns for all  $t = 1$  states CIB was treated exactly by taking in addition to  $T = 1/2$  also  $T = 3/2$  states and the corresponding  $t_{np}$  and  $t_{nn}$  t-matrices

1	2	3	4	5	6	7	8	9
$E_{lab}$ [MeV]	no CIB $V_{123} = 0$ $^1S_0$ np	no CIB $V_{123} = 0$ $^1S_0$ nn	no CIB $V_{123} = 0$ $t_{\text{eff}}$	no CIB $V_{123}$ $t_{\text{eff}}$	$^1S_0$ CIB $V_{123} = 0$	$^1S_0$ CIB $V_{123}$	CIB $V_{123} = 0$	CIB $V_{123}$
13.0	867.0	858.8	861.5	874.6	861.6	874.8	861.6	874.8
65.0	163.4	159.4	160.7	169.3	160.7	169.4	160.7	169.3
135.0	77.21	75.91	76.34	80.92	76.34	80.93	76.34	80.91
250.0	53.35	53.41	53.39	55.48	53.39	55.49	53.39	55.48

**Table 2** The nd elastic scattering total cross section (in [mb]). For the description of underlying dynamics see Table 1

1	2	3	4	5	6	7	8	9
$E_{lab}$ [MeV]	no CIB $V_{123} = 0$ $^1S_0$ np	no CIB $V_{123} = 0$ $^1S_0$ nn	no CIB $V_{123} = 0$ $t_{\text{eff}}$	no CIB $V_{123}$ $t_{\text{eff}}$	$^1S_0$ CIB $V_{123} = 0$	$^1S_0$ CIB $V_{123}$	CIB $V_{123} = 0$	CIB $V_{123}$
13.0	699.8	699.3	699.4	711.8	699.5	712.0	699.5	712.0
65.0	71.43	69.53	70.15	75.68	70.15	75.70	70.15	75.67
135.0	20.80	20.31	20.46	22.63	20.46	22.64	20.46	22.62
250.0	8.769	8.774	8.769	9.472	8.769	9.475	8.769	9.471

**Table 3** The nd breakup total cross section (in [mb]). For the description of underlying dynamics see Table 1

1	2	3	4	5	6	7	8	9
$E_{lab}$ [MeV]	no CIB $V_{123} = 0$ $^1S_0$ np	no CIB $V_{123} = 0$ $^1S_0$ nn	no CIB $V_{123} = 0$ $t_{\text{eff}}$	no CIB $V_{123}$ $t_{\text{eff}}$	$^1S_0$ CIB $V_{123} = 0$	$^1S_0$ CIB $V_{123}$	CIB $V_{123} = 0$	CIB $V_{123}$
13.0	167.2	159.8	162.1	162.9	162.1	162.8	162.1	162.9
65.0	91.92	89.89	90.58	93.69	90.58	93.69	90.58	93.61
135.0	56.42	55.60	55.88	58.29	55.88	58.29	55.88	58.28
250.0	44.58	44.64	44.62	46.01	44.62	46.01	44.62	46.01

From Tables 1, 2, and 3 it is clear that it is sufficient to use the effective t-matrix  $t_{\text{eff}}$  and to neglect  $T = 3/2$  states completely to account exactly for CIB effects in all three total cross sections. That is true in both cases, when the 3NF is present or absent. In the case when the 3NF is not included, the total cross sections for the nd interaction, for elastic scattering, and for breakup, depend slightly on the  $^1S_0$  t-matrix used in the calculations. Changing it from  $t_{np}$  to  $t_{nn}$  leads to differences of the cross section values up to  $\approx 2\%$  (columns 2 and 4). Using in the  $^1S_0$  channel the effective t-matrix  $t_{\text{eff}} = (2/3)t_{nn} + (1/3)t_{np}$  accounts for all CIB effects exactly, without the necessity to introduce the total isospin  $T = 3/2$  components in any of the  $t = 1$  partial wave states. Namely, the exact treatment of CIB by using in all  $t = 1$  states the  $t_{np}$  and  $t_{nn}$  t-matrices and both  $T = 1/2$  and  $T = 3/2$  partial wave states (column 8) gives the same value for all three total cross sections. Also restricting the exact treatment of CIB to the  $^1S_0$  state only (column 6) provides the same values for the total cross sections. It shows that contribution of  $T = 3/2$  states, as far as the total cross sections are concerned, can be neglected and all CIB effects properly taken into account by restricting to the total isospin  $T = 1/2$  states only and using in all  $t = 1$  channels the effective t-matrix generated according to the “2/3 – 1/3” rule.

The same is true when 3NF is included. In this case, in all three total cross sections, clear effects increasing with energy are seen. But again, all three treatments of CIB yield the same numbers (columns 5, 7, and 9). Since in the cases when  $T = 3/2$  states were included (columns 7 and 9) also the corresponding  $T = 3/2$  matrix elements of a 3NF were used, we conclude that their influence on the total cross sections is negligible.

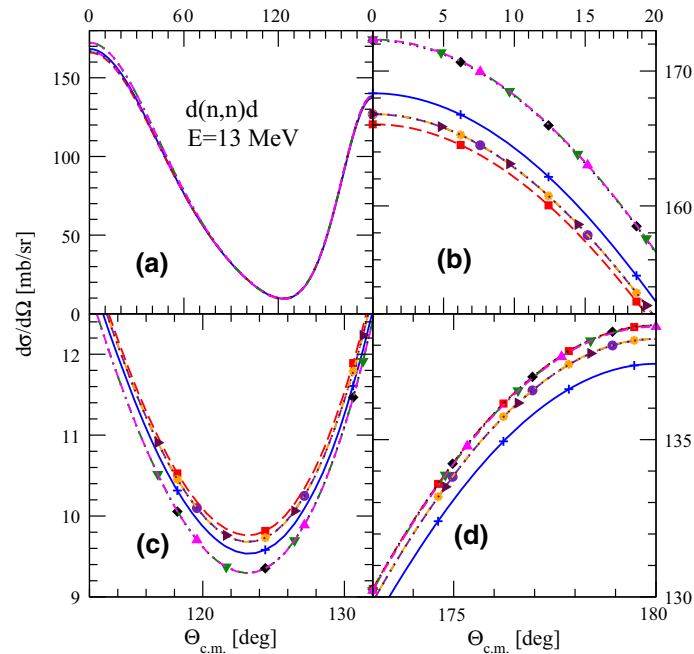


**Fig. 3** (Color online) The nd elastic scattering cross section at 13 MeV of the incoming neutron laboratory energy. In **a** the full angular distribution is shown while in **b**, **c** and **d** the forward, intermediate and backward regions of angles are displayed. *Different lines and symbols* lying on them are predictions obtained with the locally regularized (regulator  $R = 0.9$  fm)  $N^4$ LO NN potential alone or combined with the locally regularized  $N^2$ LO 3NF force for different underlying dynamics: *short-dashed (circles indigo) line*—NN potential alone and in all  $t = 1$  states effective t-matrix  $t_{\text{eff}}$  was used, *solid (pluses: blue) line*—NN potential alone, in the  $^1S_0$  state np force and in all other  $t = 1$  states the effective t-matrix  $t_{\text{eff}}$  was used, *dashed (squares: red) line*—NN potential alone, in the  $^1S_0$  state the nn force and in all other  $t = 1$  states the effective t-matrix  $t_{\text{eff}}$  was used, *dotted (diamonds: black) line*—NN potential combined with 3NF and in all  $t = 1$  states the effective t-matrix  $t_{\text{eff}}$  was used, *dashed-dotted (stars: orange) line*—NN potential alone, in the  $^1S_0$  channels np and nn forces with isospin  $T = 3/2$  included and in all other  $t = 1$  states the effective t-matrix  $t_{\text{eff}}$  was used, *dotted (triangles right: maroon) line*—NN potential alone, in all  $t = 1$  states np and nn forces used and isospin  $T = 3/2$  included, *dashed-double-dotted (triangles down: green) line*—NN potential combined with 3NF, in  $^1S_0$  states the np and nn forces used and isospin  $T = 3/2$  included and in all other  $t = 1$  states the effective t-matrix  $t_{\text{eff}}$  was used, *dotted-double-dashed (triangles up: magenta) line*—NN potential combined with 3NF, in all  $t = 1$  states the np and nn forces used and isospin  $T = 3/2$  states included

### 3.1 Elastic Scattering

In Figs. 3 and 4 we display results for the nd elastic scattering angular distributions obtained using different assumptions about the underlying dynamics and treatment of CIB. To improve the readability of the figures we put on each line a unique symbol of the same color as the line. As for the total cross sections, in case when the 3NF is inactive, the three treatments of the CIB, namely using  $t_{\text{eff}}$  and no  $T = 3/2$  states,  $T = 3/2$  in the  $^1S_0$  state with the  $t_{np}$  and  $t_{nn}$  t-matrices in that state, and  $T = 3/2$  in all  $t = 1$  states with the corresponding np and nn t-matrices, provide the same elastic scattering cross sections (short-dashed (circle: indigo), dashed-dotted (star: orange), and dotted (triangle right: maroon) lines, respectively). These lines overlap in Figs. 3 and 4 and the results are displayed in more detail in (b), (c), and (d) for particular ranges of angles. We checked that also for all nd elastic scattering spin observables, encompassing the neutron (vector) and deuteron (vector and tensor) analyzing powers, the spin correlation as well as spin transfer coefficients, the above three approaches lead to the same results. Thus again the contribution of all  $T = 3/2$  states can be neglected and CIB in elastic nd scattering treated exactly by restricting only to  $T = 1/2$  states and using in all  $t = 1$  states the “ $2/3 - 1/3$ ” rule to generate from  $t_{np}$  and  $t_{nn}$  the effective  $t_{\text{eff}}$  t-matrix.

Restricting to  $t_{np}$  or  $t_{nn}$  t-matrices in the  $^1S_0$  channel and neglecting all  $T = 3/2$  states changes the elastic scattering cross sections and spin observables by up to  $\approx 1\%$  (see the solid (plus: blue) and dashed (square: red) lines, respectively, in Figs. 3 and 4).

Adding the 3NF changes the elastic scattering cross section. The 3NF effects grow with the projectile energy and are especially large in the region of intermediate and backward angles. But again the three approaches



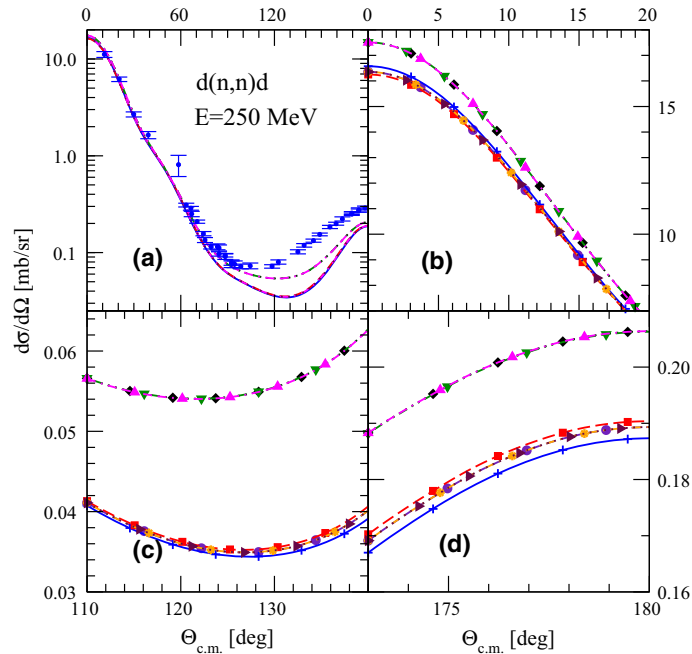


**Fig. 4** (Color online) The same as in Fig. 3 but at 250 MeV. The *solid (blue) dots* in Fig. 4a are nd data from Ref. [22]

to CIB provide the same cross sections and spin observables (they are displayed for cross sections in Figs. 3 and 4 by overlapping lines: dotted (diamond: black), dashed-double-dotted (triangle down: green), and dotted-double-dashed (triangle up: magenta)). That again supports the conclusion that  $T = 3/2$  states can be neglected together with the  $T = 3/2$  3NF matrix elements for all nd elastic scattering observables.

### 3.2 Breakup Reaction

In the final breakup state of three free nucleons both  $T = 1/2$  and  $T = 3/2$  total isospin components are allowed. Thus one would expect that here the influence of the  $T = 3/2$  components will be better visible than in elastic scattering.

We show in Figs. 5, 6, 7 and 8 that this indeed is the case for the example of three kinematically complete breakup configurations: final-state-interaction (FSI), quasi-free-scattering (QFS), and symmetrical-space-star (SST).

In the FSI configuration under the exact FSI condition, the two outgoing nucleons have equal momenta. Their strong interaction in the  $^1S_0$  state leads to a characteristic cross section maximum occurring at the exact FSI condition, the magnitude of which is sensitive to the  $^1S_0$  scattering length. Since largest CIB effects are seen in the difference between np and nn (pp)  $^1S_0$  scattering lengths, the region of the FSI peak should reveal largest CIB effects. That is clearly demonstrated in Fig. 5a for the nn and in Fig. 5b for the np FSI configuration, where the solid (plus: blue) and dashed (square: red) lines display FSI cross sections obtained with the  $^1S_0$  np and nn  $t$ -matrices, respectively, using in all other  $t = 1$  states the effective  $t$ -matrix  $t_{\text{eff}}$ . Only  $T = 1/2$  states were used and the 3NF was omitted. Using also in the  $^1S_0$  state the effective  $t$ -matrix leads to the short-dashed (circle: indigo) line, which changes to the dotted (diamond: black) line when, keeping the rest unchanged, the 3NF is also included. Most interesting is the effect of treating the CIB exactly in the state  $^1S_0$  by including the  $T = 3/2$  component and using both  $t_{np}$  and  $t_{nn}$   $t$ -matrices: dashed-dotted (star: orange) and dashed-double-dotted (triangle down: green) lines in case when 3NF is omitted and included, respectively. As expected, the inclusion of the isospin  $T = 3/2$  in the  $^1S_0$  state brings the predictions, in the case when 3NF is omitted, close to the nn prediction (dashed (square: red) line in Fig. 5a) for the nn FSI, and close to the np prediction (solid (plus: blue) line in Fig. 5b) for the np FSI. However, a significant difference exists between that result and the pure nn or np ones as well as when compared to results obtained with the effective  $t$ -matrix  $t_{\text{eff}}$  (short-dashed (circle: indigo) line in Fig. 5a, b). This shows that the proper treatment of CIB in the FSI configurations of the nd breakup requires the inclusion of the total isospin  $T = 3/2$  component and using

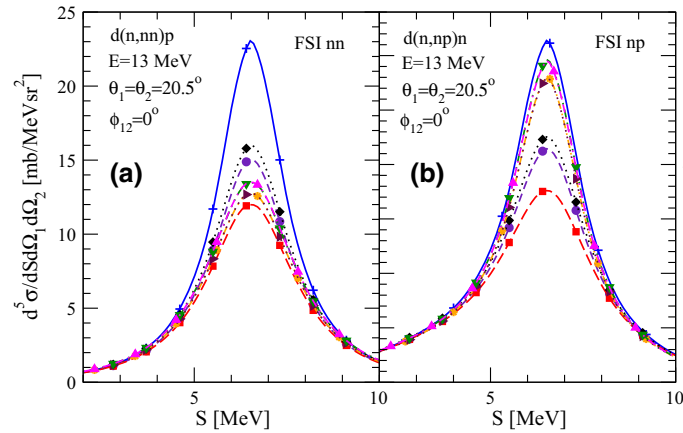


**Fig. 5** (Color online) The nd complete breakup  $d(n, nn)p$  cross section  $d^5\sigma/d\Omega_1 d\Omega_2 dS$  for the nn (a) and np (b) FSI configuration at 13 MeV of the incoming neutron laboratory energy and laboratory angles of detected outgoing nucleons  $\theta_1 = \theta_2 = 20.5^\circ$  and  $\phi_{12} = 0^\circ$ , as a function of the arc-length of the S-curve. For the description of *lines* and *symbols* see Fig. 3

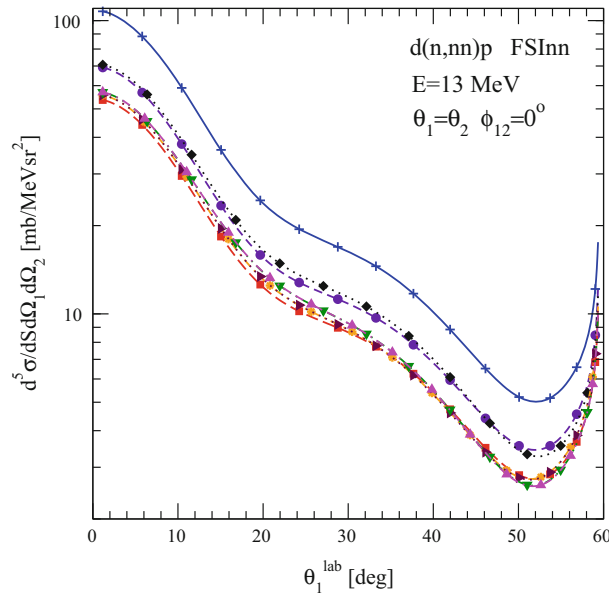


**Fig. 6** (Color online) The nd complete breakup  $d(n, nn)p$  cross section  $d^5\sigma/d\Omega_1 d\Omega_2 dS$  calculated exactly at the neutron–neutron final state interaction condition (maximum of the cross section along the S-curve) at 13 MeV of the incoming neutron laboratory energy as a function of the laboratory production angle of the outgoing final-state-interacting neutrons  $\theta_1^{lab} = \theta_2^{lab}$  and  $\phi_{12} = 0^\circ$ . For the description of *lines* and *symbols* see Fig. 3

both  $t_{np}$  and  $t_{nn}$   $t$ -matrices in the  $^1S_0$  state. This is also sufficient for the exact treatment of CIB as shown by the results of the full CIB treatment, where in all  $t = 1$  partial waves also isospin  $T = 3/2$  states are taken into account and corresponding  $t_{np}$  and  $t_{nn}$   $t$ -matrices are used, as shown in Fig. 5a, b by the dotted (triangle right: maroon) line for the NN interaction acting alone and dotted-double-dashed (triangle up: magenta) line when combined with the 3NF, respectively. These lines overlap with the lines corresponding to the case when  $T = 3/2$  is included for the state  $^1S_0$ . It is interesting to note that the  $T = 3/2$  component in the  $^1S_0$  state is important and provides FSI cross sections which are different from the results obtained with particular NN  $^1S_0$  interactions only (np for np FSI and nn for nn FSI). It proves the importance of including  $T = 3/2$  in the  $^1S_0$  state and shows that both np and nn interactions have to be employed when the FSI peaks are analyzed to extract the value of the corresponding scattering length.

In order to see how the magnitude of the effects induced by the  $T = 3/2$   $^1S_0$  component depends on the particular FSI configuration, we present in Fig. 6 the cross section in the maximum of the FSI peak as a function of the laboratory production angle of the final-state interacting pair. Again it is clearly seen that restricting to

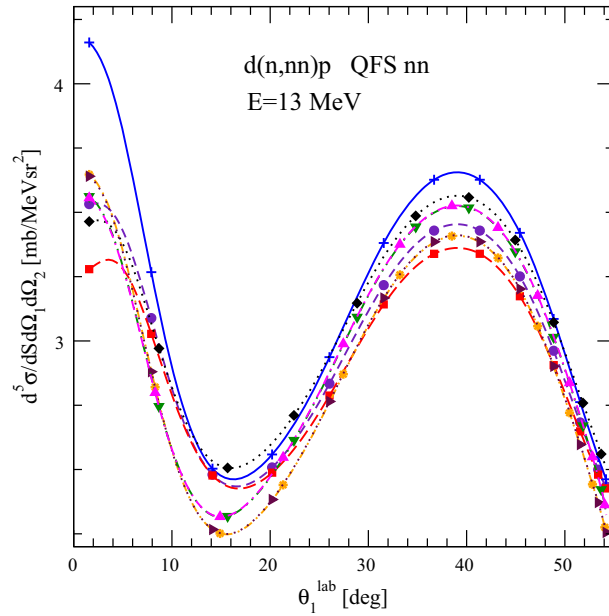


**Fig. 7** (Color online) The nd complete breakup  $d(n,nn)p$  cross section  $d^5\sigma/d\Omega_1 d\Omega_2 dS$  calculated exactly at the neutron–neutron quasi-free-scattering condition (maximum of the cross section along the S-curve at  $E_3^{lab} = 0$  and  $\phi_{12} = 180^\circ$ ) at 13 MeV of the incoming neutron laboratory energy as a function of the laboratory angle of the outgoing neutron 1. For the description of *lines* and *symbols* see Fig. 3

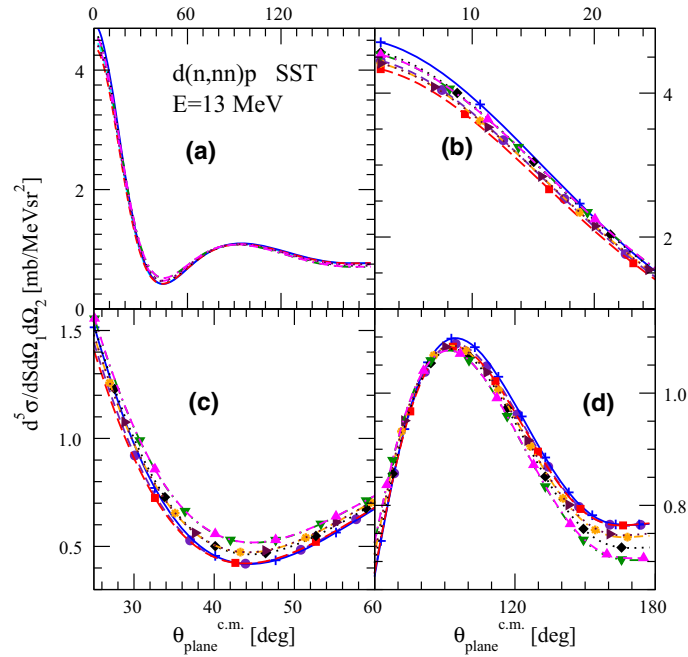


**Fig. 8** (color online) The nd complete breakup  $d(n,nn)p$  cross section  $d^5\sigma/d\Omega_1 d\Omega_2 dS$  exactly at the symmetrical-space-star condition (in the 3N c.m. system the momenta of three outgoing nucleons are equal and form a symmetric star in a plane inclined at an angle  $\theta_{\text{plane}}^{\text{c.m.}}$  with respect to the incoming neutron momentum) at 13 MeV of the incoming neutron laboratory energy, as a function of the angle  $\theta_{\text{plane}}^{\text{c.m.}}$ . For the description of lines and symbols see Fig. 3

$t_{\text{eff}}$  only and neglecting  $T = 3/2$  components is insufficient to include all CIB effects. Inclusion of  $T = 3/2$  component only in the  $^1S_0$  state is, however, sufficient to fully account for the CIB effects. The importance of that component depends on the production angle. At the angles in the region around  $\approx 45^\circ$  the contribution of that component is tiny but becomes significant at smaller and larger production angles.

For the QFS and SST configurations the picture is similar. Again in order to fully account for the CIB effects it is necessary and sufficient to include the total isospin  $T = 3/2$  component in the  $^1S_0$  state. We exemplify this in Fig. 7 for the nn QFS and in Fig. 8 for the SST configurations. Again there is an angle around which the contribution of that component is minimized. For the nn QFS it occurs around  $\theta_1^{lab} \approx 28^\circ$  and for the SST around  $\theta_{plane}^{c.m.} \approx 90^\circ$ .

## 4 Summary

We investigated the importance of the scattering amplitude components with the total 3N isospin  $T = 3/2$  in two 3N reactions. The inclusion of these components is required to account for CIB effects of the NN interaction. The difference between np and nn (pp) forces leads to a situation in which also the matrix elements of the 3NF between  $T = 3/2$  states contribute to the considered 3N reactions. The modern NN interactions, which describe existing pp and np data with high precision, provide pp and np t-matrices which differ up to  $\approx 10\%$ . Such a magnitude of CIB requires that the isospin  $T = 3/2$  components are included in the calculation of the breakup reaction, especially for the regions of the breakup phase-space close to the FSI condition. However, in order to account for all CIB effects it is sufficient to restrict the inclusion of  $T = 3/2$  to the  $^1S_0$  partial wave state only instead of doing it in all  $t = 1$  states. For elastic scattering we found that the  $T = 3/2$  components can be neglected completely and all CIB effects are accounted for by restricting oneself to total 3N isospin  $T = 1/2$  partial waves only and using the effective t-matrix generated with the “ $2/3 - 1/3$ ” rule  $t_{\text{eff}} = (2/3)t_{nn} + (1/3)t_{np}$ . These results allow one to reduce significantly the number of partial waves in time-consuming 3N calculations. This is of particular importance in view of the necessity to fix the parameters of the higher-order chiral 3NF components by fitting them to 3N scattering observables.

The presented results show that in 3N reactions the  $T = 3/2$  components are overshadowed by the dominant  $T = 1/2$  contributions. It will be interesting to investigate reactions with three nucleons in which only  $T = 3/2$  components contribute in the final state such as e.g.  $^5\text{H} + \pi^- \rightarrow n + n + n$ . That will allow one to study the properties and the importance of 3NFs in the  $T = 3/2$  states.

**Acknowledgments** This work was performed by the LENPIC collaboration with support from the Polish National Science Center under Grant No. DEC-2013/10/M/ST2/00420 and PRELUDIUM DEC-2013/11/N/ST2/03733, BMBF (Contract No. 05P2015 - NUSTAR R&D), and ERC Grant No. 307986 STRONGINT. The numerical calculations have been performed on the supercomputer cluster of the JSC, Jülich, Germany.

**Open Access** This article is distributed under the terms of the Creative Commons Attribution 4.0 International License (<http://creativecommons.org/licenses/by/4.0/>), which permits unrestricted use, distribution, and reproduction in any medium, provided you give appropriate credit to the original author(s) and the source, provide a link to the Creative Commons license, and indicate if changes were made.

## References

- Schori, O., Gabioud, B., Joseph, C., Perroud, J.P., Rügger, D., Tran, M.T., Truöl, P., Winkelmann, E., Dahme, W.: Measurement of the neutron–neutron scattering length  $a_{nn}$  with the reaction  $\pi d \rightarrow nn\gamma$  in complete kinematics. *Phys. Rev. C* **35**, 2252–2257 (1987)
- de Téramond, G.F., Gabioud, B.: Charge asymmetry of the nuclear interaction and neutron–neutron scattering parameters. *Phys. Rev. C* **36**, 691–701 (1987)
- Wiringa, R.B., Stoks, V.G.J., Schiavilla, R.: Accurate nucleon–nucleon potential with charge-independence breaking. *Phys. Rev. C* **51**, 38–51 (1995)
- Machleidt, R., Sammarruca, F., Song, Y.: Nonlocal nature of the nuclear force and its impact on nuclear structure. *Phys. Rev. C* **53**, R1483–1487 (1996)
- Stoks, V.G.J., Klomp, R.A.M., Terheggen, C.P.F., de Swart, J.J.: Construction of high-quality NN potential models. *Phys. Rev. C* **49**, 2950–2963 (1994)
- Epelbaum, E.: Few nucleon forces and systems in chiral effective field theory. *Prog. Part. Nuclear Phys.* **57**, 654–741 (2006)
- Epelbaum, E., Hammer, H.W., Meißner, U.-G.: Modern theory of nuclear forces. *Rev. Mod. Phys.* **81**, 1773–1825 (2009)
- Machleidt, R., Entem, D.R.: Chiral effective field theory and nuclear forces. *Phys. Rep.* **503**, 1–75 (2011)
- Henley, E.M., Miller, G.A.: in *Mesons and Nuclei*, Rho M. and Brown G. E., eds. (North-Holland, Amsterdam 1979). Vol. I p. 405
- Witała, H., Glöckle, W., Kamada, H.: Charge-independence breaking in the three-nucleon system. *Phys. Rev. C* **43**, 1619–1629 (1991)
- Pudliner, B.S., Pandharipande, V.R., Carlson, J.: Pieper, Steven C., Wiringa, R.B.: Quantum Monte Carlo calculations of nuclei with  $A < 7$ . *Phys. Rev. C* **56**, 1720–1750 (1997)

12. Epelbaum, E., Nogga, A., Glöckle, W., Kamada, H., Meißner, Ulf-G, Witała, H.: Three-nucleon forces from chiral effective field theory. *Phys. Rev. C* **66**, 064001–064017 (2002)
13. Epelbaum, E., Krebs, H., Meißner, U.-G.: Improved chiral nucleon–nucleon potential up to next-to-next-to-next-to-leading order. *Eur. Phys. J. A* **51**, 53–81 (2015)
14. Epelbaum, E., Krebs, H., Meißner, U.-G.: Precision nucleon–nucleon potential at fifth order in the chiral expansion. *Phys. Rev. Lett.* **115**, 122301-1-5 (2015)
15. Witała, H., Cornelius, T., Glöckle, W.: Elastic scattering and break-up processes in the  $n$ – $d$  system. *Few Body Syst.* **3**, 123–134 (1988)
16. Glöckle, W., Witała, H., Hüber, D., Kamada, H., Golak, J.: The three-nucleon continuum: achievements, challenges and applications. *Phys. Rep.* **274**, 107–285 (1996)
17. Hüber, D., Kamada, H., Witała, H., Glöckle, W.: How to include a three-nucleon force into Faddeev equations for the 3N continuum: a new form. *Acta Phys. Pol. B* **28**, 1677–1685 (1997)
18. Epelbaum, E., Meißner, U.-G., Palomar, J.E.: Isospin dependence of the three-nucleon force. *Phys. Rev. C* **71**, 024001-1-11 (2005)
19. Binder, S., et al.: Few-nucleon systems with state-of-the-art chiral nucleon–nucleon forces. *Phys. Rev. C* **93**, 044002–044006 (2016)
20. Hebeler, K., Krebs, H., Epelbaum, E., Golak, J., Skibiński, R.: Efficient calculation of chiral three-nucleon forces up to  $N^3$ LO for ab initio studies. *Phys. Rev. C* **91**, 044001–044009 (2015)
21. Witała, H., Glöckle, W., Golak, J., Nogga, A., Kamada, H., Skibiński, R., Kuroś-Żołnierczuk, J.:  $Nd$  elastic scattering as a tool to probe properties of 3N forces. *Phys. Rev. C* **63**, 024007–024012 (2001)
22. Maeda, Y., et al.: Differential cross section and analyzing power measurements for  $\vec{n}d$  elastic scattering at 248 MeV. *Phys. Rev. C* **76**, 014004–13 (2007)